Preparation and Reinforcement of Polylactic Acid/ Nanofibrillated Cellulose/ Glycidyl Methacrylate Composites

Kehong Zhang * and Wenqi Zhang

Using polylactic acid (PLA) and nanocellulose (NFC) as raw materials, and glycidyl methacrylate (GMA) as the modifier, the PLA/NFC-GMA composite was prepared by solution blending. The addition of GMA effectively improved the dispersion of NFC in PLA, with NFC being grafted onto the PLA molecular chain through a reaction with GMA. The tensile strength of PLA/NFC-GMA composites increased with NFC loading, while GMA improved interfacial compatibility and dispersion, leading to a non-monotonic strength trend and reduced elongation at break. The PLA/NFC-GMA composite with 0.7 wt.% NFC and 6.0 wt.% GMA had the best mechanical properties, with the tensile strength of 27.7 MPa and the elongation at break of 78.4%. The PLA/NFC-GMA composite exhibited excellent UV shielding. Its transmittance was nearly zero below 280 nm and it maintained high transparency within the wavelength range of 400 to 800 nm, with a transmittance exceeding 85%. The transparency of the composite reached its maximum when the NFC and GMA loadings were 0.7 and 1.5 wt.% relative to PLA, respectively. GMA significantly enhanced the thermal stability of PLA/NFC-GMA composites. The thermal stabilization effect of GMA became saturated at ~3.0 wt.%, beyond which additional GMA primarily promoted more complete volatilization without further improving thermal resistance.

DOI: 10.15376/biores.21.4.9910-9920

Keywords: Polylactic Acid; Nanofibrillated Cellulose; Methyl methacrylate glycidyl; Graft modification

*Contact information: Anhui Engineering Research Center for Highly Functional Fiber Products for Automobiles, College of Materials and Chemistry, Anhui Agricultural University, Hefei, Anhui 230036, China; * Corresponding author: zkh@ahau.edu.cn*

INTRODUCTION

As the "white pollution" caused by non-biodegradable waste plastics becomes increasingly severe, and with the gradual depletion of fossil fuel resources, global environmental challenges are intensifying. The development of sustainable and biodegradable polymers has thus become a crucial task. Poly(lactic acid) (PLA), derived from renewable biomass such as corn starch and sugarcane, exhibits superior tensile strength, optical clarity, and thermoplastic processability. These attributes position it as a premier candidate for packaging, biomedical, and agricultural applications (Farah *et al.* 2022). However, its broad commercial adoption is hindered by inherent deficiencies, including high brittleness, sluggish crystallization kinetics, low heat distortion temperature, and poor impact resistance (Nofar *et al.* 2019). To address these limitations, various strategies such as physical blending, chemical copolymerization, plasticization, and nanofiller reinforcement have been extensively investigated (Xu *et al.* 2021). Notably, the

incorporation of nanoscale reinforcements has emerged as a potent strategy to synergistically enhance mechanical toughness, thermal stability, and functional performance without compromising biodegradability (Habibi *et al.* 2010; Hubbe *et al.* 2021).

Derived from sustainable lignocellulosic sources, nanofibrillated cellulose (NFC) particle exhibit a unique hierarchical architecture with high aspect ratios and exceptional mechanical properties (Klemm *et al.* 2022). These attributes, coupled with a reactive hydroxylated surface, position NFC as a premier candidate for reinforcing biopolymer matrices (Nechyporchuk *et al.* 2016). In particular, PLA/NFC composites offer a promising route toward fully renewable materials with tailored performance (Zhang *et al.* 2024). While well-dispersed NFC can effectively modulate PLA crystallization and stress transfer, the fundamental polarity mismatch between hydrophilic NFC and hydrophobic PLA poses a significant hurdle (Jonoobi *et al.* 2021). The polarity mismatch and the difference in hydrogen bonding ability triggers NFC aggregation, leading to detrimental phase separation and stress concentration sites (Dufresne 2013). Such issues compromise the synergistic potential of the composite, particularly regarding optical transparency and thermal stability. Thus, engineering a seamless interface with uniform nanofibrillar dispersion remains a critical bottleneck for the next generation of high-performance PLA biocomposites.

To overcome the interfacial incompatibility between hydrophilic nanocellulose and hydrophobic polymer matrices, the strategic incorporation of compatibilizers has proven highly effective. Compatibilizers generally operate by reducing interfacial tension, suppressing filler aggregation, and facilitating efficient stress transfer across the matrix–reinforcement boundary (Zhang *et al.* 2023). A variety of compatibilizing agents have been investigated, including block copolymers, organosilanes, maleic anhydride-grafted polymers, and reactive epoxy-functionalized monomers (Li and Zhang 2024). Among these, glycidyl methacrylate (GMA) has emerged as a particularly potent reactive compatibilizer owing to its bifunctional molecular architecture. The epoxy moiety readily undergoes ring-opening reactions with surface hydroxyl groups on NFC, establishing stable covalent linkages, while the methacrylate segment can physically entangle with or form favorable intermolecular interactions with PLA chains (Zhao *et al.* 2021). This dual-action mechanism not only mitigates NFC agglomeration but also constructs a continuous interfacial network that enhances load-bearing capacity, improves ductility, and stabilizes thermal degradation pathways (Kalia *et al.* 2011). Contemporary studies confirm that GMA-mediated reactive compatibilization can significantly elevate the thermo-mechanical performance of biopolymer nanocomposites while maintaining their environmental degradability (Wu and Habibi 2017).

Based on the above considerations, this work aims to fabricate PLA/NFC-GMA composites *via* solution blending using chloroform ($CHCl_3$) as solvent, with NFC as reinforcement, PLA as matrix, and GMA as reactive compatibilizer. The mechanistic feasibility of this approach hinges on the *in-situ* interfacial engineering wherein GMA grafts onto NFC surfaces *via* epoxy–hydroxyl reactions, and the grafted molecular chains subsequently interpenetrate and interact with the PLA matrix, thereby constructing a robust stress-transfer network. By systematically adjusting the loadings of NFC and GMA, the microscopic morphology, mechanical properties, light transmittance, and thermal stability of the composites were characterized. The underlying mechanism of the interfacial reaction and its impact on the macro-performance were elucidated through FTIR and SEM analysis. This research aimed to provide a theoretical basis and technical support for the preparation

of high-performance, transparent, and fully biodegradable materials, contributing to the high-value utilization of biomass resources in sustainable packaging applications.

EXPERIMENTAL

Materials

Polylactic acid (PLA), catalogue number 4032D, was purchased from NatureWorks LLC. (Inglewood, Colorado, USA). The nano-cellulose suspension NFC-B5 (NFC) was provided by Zhejiang Jinjiahao Green Nanomaterials Co., Ltd. (Quzhou, China), with a mass fraction of 10 wt.%, a diameter of 3 to 30 nm, and a length of 50 to 300 nm. Trichloromethane ($CHCl_3$) was purchased from Fuchen Chemical Reagent Co., Ltd. (Tianjin, China). Glycidyl methacrylate (GMA) was purchased from Tianjin Xishensheng Biochemical Technology Co., Ltd. (Tianjin, China). All reagents were of analytical grade and were not further purified for use.

Preparation of PLA/NFC Composite

The PLA was dried in a DHG-92022A oven at 60 °C for 12 h and stored for subsequent use. A 10 wt.% NFC solution was frozen at −5 °C for 24 h, followed by freeze-drying in an FD-1A-50 freeze dryer for 24 h to obtain NFC powder. Then, 40 mL of chloroform was measured into a beaker, into which the NFC powder was added. The suspension was sonicated at room temperature for 30 min using an XLW-PC ultrasonic cell disruptor at a power of 1000 W to yield a uniformly dispersed NFC/chloroform suspension. Subsequently, GMA was added dropwise to the NFC dispersion under magnetic stirring for 4 h to achieve GMA modification of the NFC. Next, 1.6 g of PLA was added, and the mixture was stirred at 40 °C for 0.5 h, followed by an additional 30 min of sonication to prepare a homogeneous PLA/NFC blend solution. The resulting solution was poured into a petri dish and dried at room temperature in a fume hood for 12 h to obtain PLA/NFC composite films. The mass fractions of NFC relative to PLA were set at 0.1 wt.%, 0.3 wt.%, 0.5 wt.%, and 0.7 wt.%, while the GMA dosages were 1.5 wt.%, 3.0 wt.%, 4.5 wt.%, and 6.0 wt.% (based on the mass of PLA). These composite materials were designated as PLA/NFC-x-GMA-y, where x and y represent the mass percentages of NFC and GMA relative to PLA, respectively.

Characterizations

After being frozen in liquid nitrogen and subsequently fractured, the cross-sections of the PLA/NFC composite films were sputter-coated with a thin gold layer and then examined for cross-sectional morphology using an S-4800 scanning electron microscope (SEM) at an accelerating voltage of 1.0 kV.

The infrared absorbance spectra of all samples were recorded on a TENSOR II spectrometer (Bruker Corporation, Karlsruhe, Germany) over the wavenumber range of 500 to 4000 cm^{-1}, with a spectral resolution of 4 cm^{-1} and 32 scans per sample.

The tensile properties of dumbbell-shaped specimens were evaluated in accordance with ASTM D882 using an ASR-1024 electronic universal testing machine (Guangdong AISRY Instrument Technology Co., Ltd, Dongguan, China) with the tensile speed of 50 mm/min (the length × width of samples was 50 mm × 4 mm). The results for mechanical properties were reported as the average of 5 samples.

The transmittance properties of the samples (the length × width of samples was 50 mm × 15 mm) were tested using an UV/V-16/18 ultraviolet/visible spectrophotometer (Shanghai Yiheng Scientific Instrument Co., Ltd., Shanghai, China) within the wavelength range of 200 to 800 nm, with an interval of 20 nm. The transmittance properties were the average of 3 samples.

The hydrophobicity of the samples was evaluated by measuring the water contact angle (WCA) using a JC2000D38 contact angle goniometer (Shanghai Zhongchen Digital Technology Equipment Co., Ltd., Shanghai, China). All reported values represent the mean of 3 samples.

Thermogravimetric analysis (TGA) was conducted on a TGA/DSC 1/1100 thermal analyzer (Mettler Toledo International Inc., Zürich, Switzerland) to assess the thermal stability of the samples. Tests were carried out under a continuous nitrogen flow (20 mL/min) from 50 to 600 °C with a constant heating rate of 10 °C/min.

RESULTS AND DISCUSSION

SEM Analysis

To evaluate the effects of NFC and GMA loading on the composite morphology, SEM analysis was performed on PLA/NFC-0.3, PLA/NFC-0.7, PLA/NFC-0.3-GMA-3.0, and PLA/NFC-0.7-GMA-6.0 samples, as shown in Fig. 1. The tensile fracture surface of the PLA/NFC-0.3 composite appeared rough, with evident fiber pull-out and void formation. Such characteristics indicate typical brittle fracture behavior in polymers (Fig. 1a). With the increase in NFC content, the tensile fracture surface of the PLA/NFC-0.7 composite exhibited characteristics of ductile fracture, but NFC showed agglomeration (Fig. 1b).

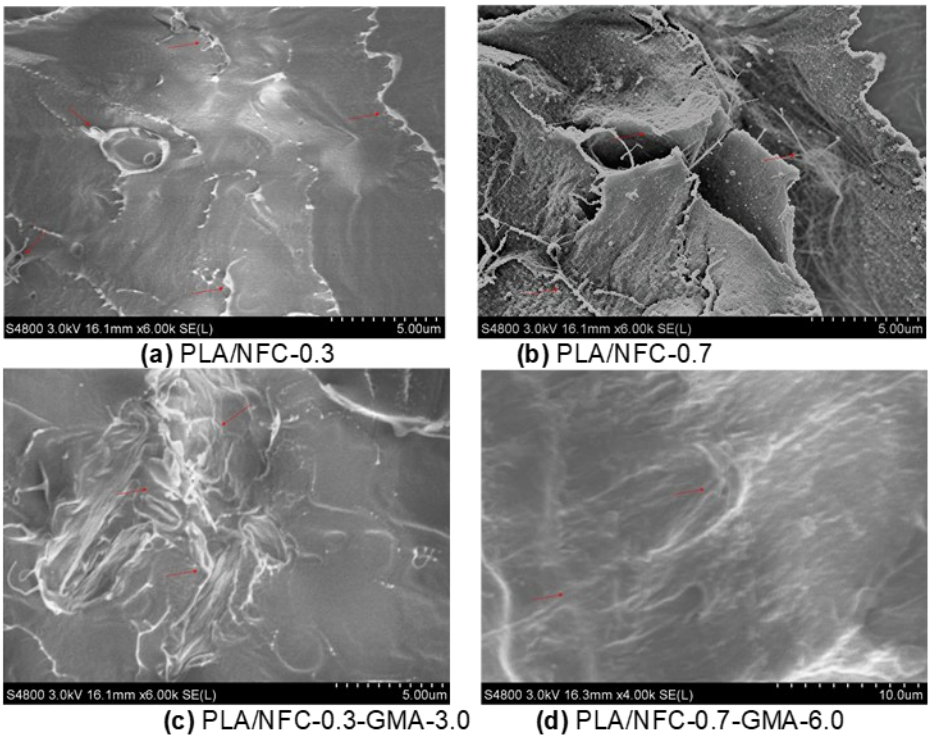

Fig. 1. SEM images of PLA/NFC/GMA with different NFC and GMA content

In contrast, the fracture surface of the PLA/NFC-0.3-GMA-3.0 film (Fig. 1c) displayed numerous tear-like features, with no observable NFC agglomeration. This suggests that the modified NFC effectively hindered rapid crack propagation and enhanced stress dissipation within the PLA matrix. For the PLA/NFC-0.7-GMA-6.0 composite (Fig. 1d), the fracture morphology exhibited clear ductile fracture characteristics, densely populated with crazes and devoid of significant filler agglomeration. These observations confirm that NFC modification strengthened the interfacial adhesion with the PLA matrix, thereby imparting a pronounced toughening effect and contributing to the overall enhancement of the composite's mechanical properties.

FTIR Analysis

Figure 2 displays the FTIR spectra of NFC, PLA, PLA/NFC-0.3, and PLA/NFC-0.7-GMA-6.0 composite films. For neat PLA, characteristic absorbance peaks at 1747 and 1080 cm^{-1} were assigned to the C=O and C-O stretching vibrations of the ester groups in the PLA backbone, respectively. The NFC spectrum exhibited a broad absorbance peak centered at approximately 3400 cm^{-1}, corresponding to O-H stretching vibrations of cellulose hydroxyl groups, along with a characteristic peak at 1120 cm^{-1} attributed to C-O-C asymmetric stretching of cellulose glycosidic linkages. The PLA/NFC-0.3 blend spectrum revealed a simple superposition of individual PLA and NFC features, suggesting predominantly physical mixing with minimal chemical interaction between phases. In contrast, the PLA/NFC-0.7-GMA-6.0 composite exhibited distinct spectral modifications indicative of successful interfacial coupling *via* GMA.

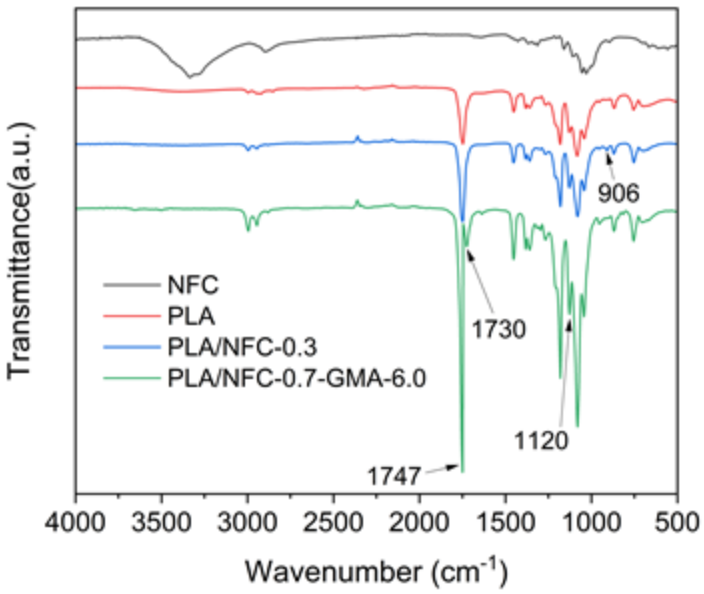

Fig. 2. FTIR spectra of NFC, PLA and PLA/NFC-GMA composite film

Notably, a new absorbance peak appeared at 1730 cm^{-1}, corresponding to the ester carbonyl stretching vibration of the grafted GMA groups, which differed from the ester peak of PLA (1747 cm^{-1}). Crucially, compared to PLA/NFC-0.3, the characteristic epoxy peak at 906 cm^{-1} was absent in PLA/NFC-0.7-GMA-6.0, indicating that the GMA epoxy ring had opened to react with the NFC hydroxyl groups, thereby achieving the grafting of PLA onto NFC. These spectral features suggest that GMA acts as a reactive compatibilizer

through nucleophilic ring-opening reactions between its epoxy groups and hydroxyl functionalities on both NFC surfaces and PLA chain termini, forming covalent ether and ester linkages. This chemical bridging mechanism significantly enhances interfacial adhesion between the hydrophilic NFC and hydrophobic PLA matrix, thereby facilitating efficient stress transfer and contributing to the superior mechanical performance observed in GMA-compatibilized composites.

Mechanical Properties

Mechanical properties are crucial indicators for evaluating composite performance. The tensile strength and elongation at break of PLA/NFC-GMA composite films with different NFC contents and different GMA contents are presented in Fig. 3. In Fig. 3(a), the tensile strength of PLA/NFC/GMA composites exhibited a progressive increase with increasing NFC loading, whereas the elongation at break demonstrated a corresponding declining trend. This behavior may be attributed to the formation of a sufficiently uniform network within the PLA matrix, which effectively facilitates stress distribution and interfacial load transfer, thereby reinforcing the mechanical performance of the PLA-based composites. Nevertheless, the incorporation of NFC may simultaneously disrupt the inherent structural integrity of the PLA matrix and impede the segmental mobility of PLA molecular chains, leading to a reduction in elongation at break. Furthermore, such constraining effects became increasingly pronounced at higher NFC loadings. Figure 3(b) presents the effect of GMA content on the tensile properties of PLA/NFC/GMA composites at a fixed NFC loading of 0.7 wt.%. With increasing GMA content, the tensile strength of the composites initially decreased and subsequently increased, while the elongation at break exhibited a monotonic decline throughout the investigated range. Notably, both tensile strength and elongation at break attained their minimum values at a GMA content of 3.0 wt.%. This phenomenon can be primarily ascribed to the enhanced interfacial compatibility achieved through GMA modification, which promotes homogeneous dispersion of NFC within the PLA matrix and mitigates nanoparticle agglomeration, thereby facilitating efficient stress transfer and ultimately enhancing the tensile strength of the composites. Collectively, the optimal tensile performance was achieved for PLA/NFC/GMA composites containing 0.7 wt.% NFC and 6.0 wt.% GMA, yielding a tensile strength of 27.7 MPa and an elongation at break of 78.4%.

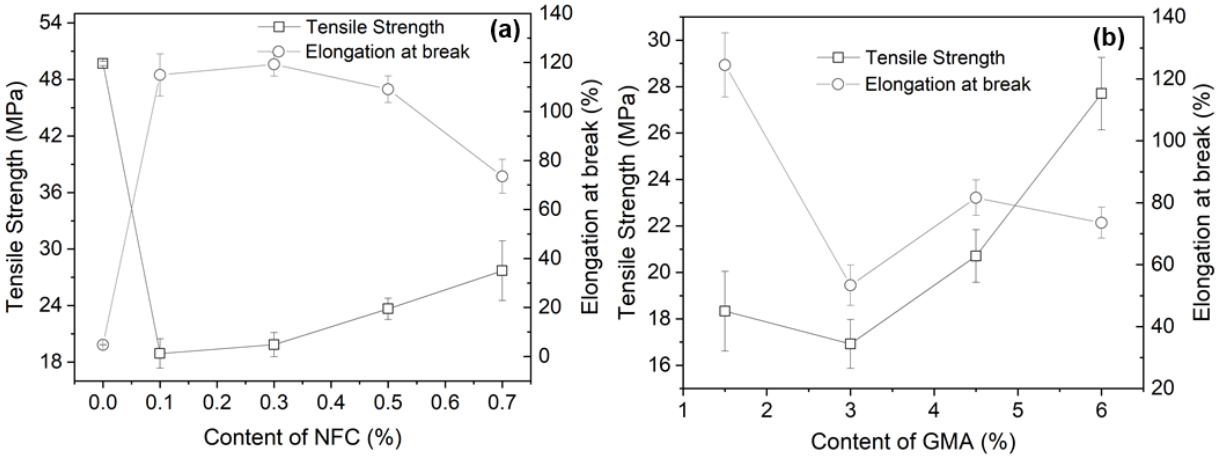

Fig. 3. The tensile properties of PLA/NFC-GMA composite films with different NFC contents (a) and different GMA contents (b)

Light Transmission Performance

Transmittance is a critical parameter influencing the practical application of film materials. To elucidate the properties of PLA/NFC-GMA composites and broaden their potential application scope, their optical transmittance was systematically evaluated. As shown in Fig. 4, all samples exhibited excellent UV-shielding performance, with near-zero transmittance below 280 nm and a pronounced absorption edge around 300 nm. At the same time, they maintained high transparency in the visible region (400 to 800 nm), with transmittance exceeding 85%. Among the samples, the PLA/NFC-0.7-GMA-1.5 composite demonstrated the highest overall transparency. In contrast, a higher GMA content (6.0 wt.%) resulted in a slight decrease in transmittance, likely due to the formation of additional light-scattering centers caused by excessive modification. The superior optical clarity was attributed to the effective refractive index matching between the PLA matrix and GMA-modified NFC, as well as the nanoscale dimensions and uniform dispersion of the fibers, which together minimize Rayleigh scattering. The inherent UV absorption originates from the chemical structure of cellulose and the ester groups within the composite. These synergistic optical properties, high visible transparency coupled with efficient UV-blocking capability, make PLA/NFC/GMA nanocomposites highly promising for applications such as transparent food packaging films.

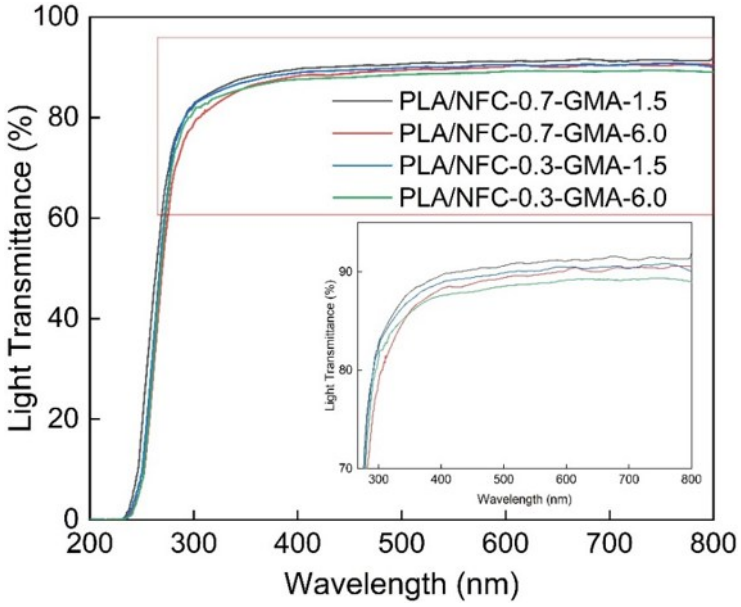

Fig. 4. The light transmittance of PLA/NFC-x-GMA-y (x=0.3, 0.7; y = 1.5, 6.0)

Thermostability

Figure 5 shows the TG and DTG curves of PLA, NFC, PLA/NFC, and PLA/NFC-0.7-GMA-3.0 composites. The thermogravimetric (TG) and derivative thermogravimetric (DTG) curves revealed distinct thermal degradation behaviors for NFC, PLA, and their composites. Neat NFC exhibited an initial minor weight loss below 120 °C. This was attributed to the evaporation of absorbed moisture, followed by a major degradation stage occurring at 280 to 350 °C, corresponding to the depolymerization of cellulose chains and the cleavage of glycosidic linkages. In contrast, neat PLA showed a single, sharp degradation step with a maximum weight loss rate at a higher temperature (350 to 380 °C), which is associated with random chain scission and the unzipping depolymerization of

ester bonds. The PLA/NFC composite displayed a slightly reduced onset degradation temperature compared to neat PLA, indicating that the incorporation of NFC accelerated thermal decomposition. This was likely due to the lower thermal stability of cellulose and the heterogeneous interfacial structure that facilitates heat transfer and degradation initiation. However, the introduction of GMA altered this behavior. The PLA/NFC-GMA composite exhibited an increased onset decomposition temperature and a shift of the DTG peak toward higher temperatures relative to PLA/NFC, suggesting enhanced thermal stability. This improvement was attributed to the reactive compatibilization effect of GMA, which promoted interfacial adhesion through possible grafting reactions between PLA and NFC, thereby restricting polymer chain mobility and delaying thermal degradation. Additionally, the reduced peak intensity in the DTG curve for PLA/NFC-GMA indicated a more gradual degradation process, further confirming the formation of a more thermally stable and structurally integrated network.

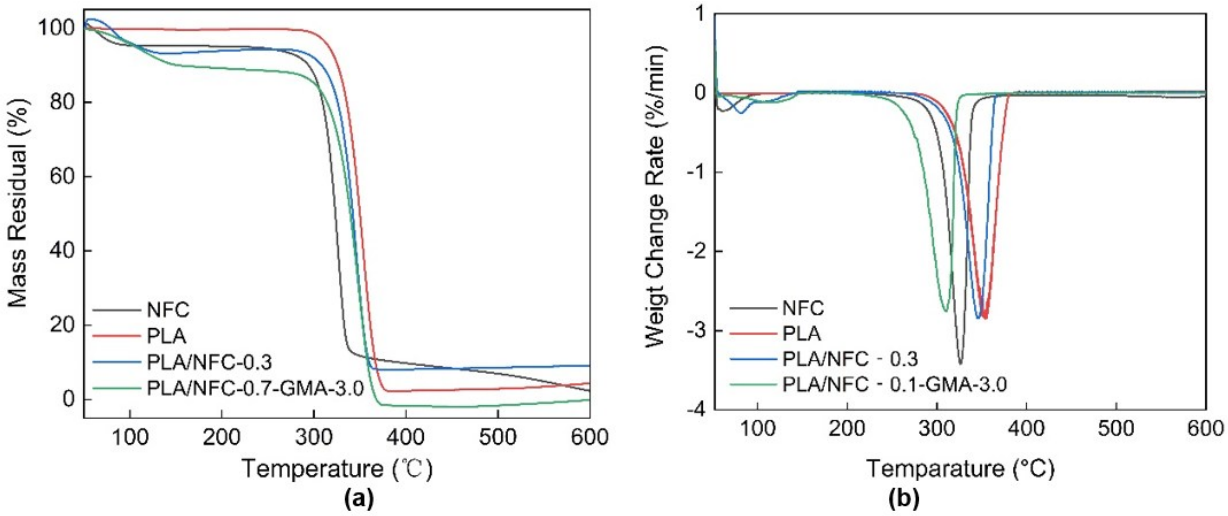

Fig. 5. TGA (a) and DTG (b) Curves of NFC, PLA, PLA/NFC and PLA/NFC-GMA

The thermal degradation behaviors of the PLA/NFC-GMA composites with varying NFC and GMA contents were investigated using TGA and DTG, as illustrated in Fig. 6. There was a major weight loss between 300 and 400 °C, which was attributed to the random chain scission of the PLA matrix and the thermal degradation of the cellulose component. The DTG curves reveal that T_{max} was affected by NFC content. The composite with the lowest NFC loading (PLA/NFC-0.1-GMA-3.0) presented the lowest onset temperature of rapid thermal decomposition T_{onset} (about 253 °C) with a sharp peak, while increasing the NFC content to 0.3 and 0.7 wt.% resulted in an upward shift of T_{onset} to around 288 °C. This enhancement in thermal stability was attributed to the barrier effect produced by well-dispersed NFC and the restriction of PLA chain segmental movement resulting from the grafting of GMA-modified NFC onto the PLA molecular chains, while the lower stability of the 0.1 wt.% sample likely stemmed from the plasticizing effect or early degradation of excess ungrafted GMA relative to the low filler content. Conversely, the residual mass at 600 °C showed an inverse dependence on NFC content, decreasing from about 8% at 0.1 wt.% NFC to about 2% at 0.7 wt.%. Excess GMA in the low-NFC system promoted char formation *via* cross-linking, whereas higher NFC loading enhanced interfacial adhesion, thereby facilitating more complete thermal volatilization.

Furthermore, when the NFC content was fixed at 0.7 wt.%, increasing the GMA content from 3.0 wt.% to 6.0 wt.% led to only a marginal variation in T_{max}, along with a slight reduction in the residual mass at 600 °C. This suggests that the compatibilization effect of GMA in enhancing thermal stability reached a saturation level at around 3.0 wt.%, beyond which additional GMA predominantly facilitates more complete volatilization of the composite during thermal degradation.

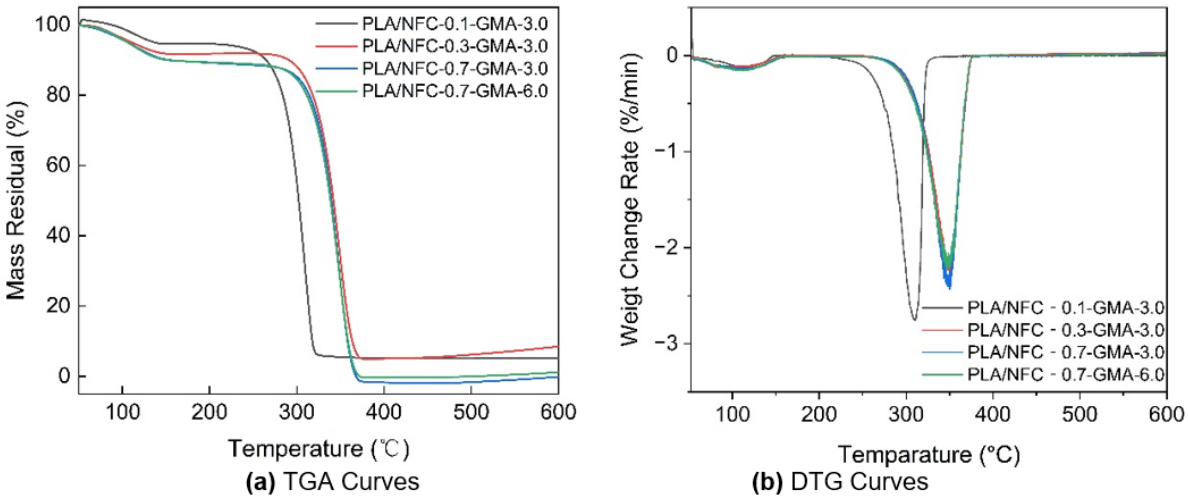

Fig. 6. The TGA (a) and DTG (b) Curves of PLA/NFC-GMA with different NFC and GMA content

CONCLUSIONS

1. Using polylactic acid (PLA) and nanocellulose (NFC) as raw materials, and glycidyl methacrylate (GMA) as the modifier, the PLA/NFC-GMA composite material was prepared by solution blending. The microstructure, mechanical properties, transmittance, hydrophilicity, and thermal stability of the composite material were characterized. The effects of NFC content and GMA dosage on the structure and properties of the PLA/NFC-GMA composites were studied. The results of scanning electron microscope (SEM) and Fourier transform infrared (FTIR) analyses indicated that the addition of GMA effectively improved the dispersion of NFC in PLA and NFC was grafted onto the PLA molecular chain.
2. The tensile strength of PLA/NFC-GMA composites progressively increased with NFC loading due to percolating network formation, while GMA incorporation enhanced interfacial compatibility and filler dispersion, resulting in a non-monotonic strength response and reduced elongation at break. The PLA/NFC-GMA composite with 0.7 wt.% NFC and 6.0 wt.% GMA had the best mechanical properties, with the tensile strength of 27.7 MPa and the elongation at break of 78.4%, demonstrating effective stress transfer and balanced reinforcement-ductility synergy.
3. The PLA/NFC-GMA composite exhibited excellent UV shielding performance. Its transmittance was nearly zero below 280 nm, and it maintained high transparency within the range of 400 nm to 800 nm, with a transmittance exceeding 85%. Among all the samples, the overall transparency of the PLA/NFC-GMA composite with 0.7 wt.%

NFC and 1.5 wt.% GMA was the highest. A higher GMA content led to a decrease in the transmittance of the PLA/NFC-GMA composite.

4. Thermogravimetric analysis demonstrated that GMA significantly enhanced the thermal stability of PLA/NFC-GMA composites. While increasing NFC content from 0.1 wt.% to 0.7 wt.% elevated the onset temperature of rapid thermal decomposition from about 253 °C to about 288 °C due to barrier effects and restricted polymer chain mobility, the residual char at 600 °C decreased inversely with NFC loading, reflecting altered degradation pathways. The thermal stabilization effect of GMA reached saturation at approximately 3.0 wt.%, beyond which additional GMA primarily facilitated more complete volatilization without further improving thermal resistance.

ACKNOWLEDGMENTS

The authors are grateful for the support of the Natural Science Research Project of Anhui Educational Committee, Grant No. 2023AH050979; the Anhui Agricultural University-Anhui Huayi Packaging Technology Co. Ltd. cooperation project, Grant No. hx23402; and Anhui Provincial Key Teaching Research Project, Grant No.2023jyxm0186.

REFERENCES CITED

Dufresne, A. (2013). "Nanocellulose: A versatile green platform: From maximizing yields to revitalizing papers," *Prog. Polym. Sci.* 38(11), 1590-1635. https://doi.org/10.1016/j.progpolymsci.2013.05.010

Farah, S., Anderson, D. G., and Langer, R. (2022). "Physical and mechanical properties of PLA, and their functions in widespread applications-A comprehensive review," *Adv. Drug. Deliver. Rev.* 185, article 114238. https://doi.org/10.1016/j.addr.2016.06.012

Habibi, Y., Lucia, L. A., and Rojas, O. J. (2010). "Cellulose nanocrystals: Chemistry, self-assembly, and applications," *Chem. Rev.* 110(6), 3479-3500. https://doi.org/10.1021/cr900339w

Hubbe, M. A., Lavoine, N., Lucia, L. A., and Dou, C. (2021). "Formulating bioplastic composites for biodegradability, recycling, and performance: A review," *BioResources* 16(1), 2021-2083. https://doi.org/10.15376/biores.16.1.Hubbe

Jonoobi, M., Oladi, R., Davoudpour, Y., Oksman, K., Dufresne, A., Hamzeh, Y., and Davoodi, R. (2021). "Recent advances in cellulose nanocrystals/nanofibers reinforced polylactic acid (PLA) composites: A review," *Carbohyd. Polym.* 251, article 117023. https://doi.org/10.1016/j.carbpol.2020.117023

Kalia, S., Dufresne, A., Cherian, B. M., Kaith, B. S., and Avérous, L. (2011). "Cellulose-based bio- and nanocomposites: A review," *Prog. Polym. Sci.* 36 (12), 1540-1557. https://doi.org/10.1016/j.progpolymsci.2011.04.005

Klemm, D., Heublein, B., Fink, H. P., and Bohn, A. (2022). "Cellulose: Fascinating biopolymer and sustainable raw material," *Angew. Chem. Int. Edit.* 61(12), article e202114567. https://doi.org/10.1002/anie.200460587

Li, J., and Zhang, L. (2024). "Reactive compatibilizers for cellulose nanofiber/polymer composites: Classification, mechanisms, and industrial prospects," *Compos. Sci.*

Technol. 247, article 110432.
Nechyporchuk, O., Belgacem, M. N., and Bras, J. (2016). Production of cellulose nanofibrils: A review of recent advances. *Ind. Crop. Prod.* 93, 2-25. https://doi.org/10.1016/j.indcrop.2016.02.016
Nofar, M., Sacligil, D., Carreau, P. J., and Heuzey, M. C. (2019). "Poly (lactic acid) blends: Processing, properties and applications," *Int. J. Biol. Macromol.* 125, 307-360. https://doi.org/10.1016/j.ijbiomac.2018.12.002
Wu, R., and Habibi, Y. (2017). "Functionalization of cellulose nanofibers with glycidyl methacrylate for highly tough and thermally stable bio-based nanocomposites," *ACS Appl. Mater. Interfaces* 9(24), 20830-20841. https://doi.org/10.1021/acsami.7b04514
Xu, H., Li, Z., and Chen, J. (2021). "Recent advances in modification strategies for enhancing the toughness and crystallization rate of polylactic acid," *Int. J. Biol. Macromol.* 189, 745-758. https://doi.org/10.1016/j.ijbiomac.2021.08.138
Zhang, H., Wu, J., and Li, Y. (2024). "Fully bio-based polylactic acid/cellulose nanofibril composites: Interfacial design and performance optimization," *Carbohyd. Polym* 324, article 121502. https://doi.org/10.1016/j.carbpol.2023.121502
Zhang, X., Liu, Y., and Sun, Q. (2023). "Interfacial engineering in biopolymer nanocomposites: Compatibilization mechanisms and performance enhancement," *Prog. Polym. Sci.* 138, article 101654. https://doi.org/10.1016/j.progpolymsci.2023.101654
Zhao, X., Wu, H., and Chen, Y. (2021). "GMA-grafted cellulose nanocrystals as reactive compatibilizers for polylactic acid: Synthesis, interfacial bonding, and mechanical reinforcement," *ACS Sustainable Chem. Eng.* 9(18), 6421-6430. https://doi.org/10.1021/acssuschemeng.1c01344

Article submitted: May 4, 2026; Peer review completed: May 31, 2026; Revised version received: July 6, 2026; Accepted: July 7, 2026; Published: August 19, 2026.
DOI: 10.15376/biores.21.4.9910-9920